MS.ID-IJPBS-8571
International Journal of Pharmacy and Biological Sciences-IJPBS™ (2025) 15 (4): 123-133
Online ISSN: 2230-7605, Print ISSN: 2321-3272
Research Article | Pharmaceutical Sciences | OA Journal | MCI Approved | Index Copernicus

Formulation, Box-Behnken Optimization, and Characterization of Iguratimod-Loaded Nanostructured Lipid Carriers for Enhanced Rheumatoid Arthritis Therapy

Amit Kumar Pandey[1*] and Amit Kumar[2]

[1*]Research Scholar, Faculty of Pharmaceutical Sciences, Motherhood University, Karaundi, Rookee, Haridwar, Uttarakhand-247661

[2]Proferssor, Faculty of Pharmaceutical Sciences, Motherhood University, Karaundi, Rookee, Haridwar, Uttarakhand-247661

Received: 02 Nov 2025/ Accepted: 20 Nov 2025 / Published online: 1 Dec 2025
*Corresponding Author Email: amitkpandey113@gmail.com

Abstract

Background: Iguratimod (IGU), a novel disease-modifying antirheumatic drug (DMARD), exhibits poor aqueous solubility and low oral bioavailability, limiting its therapeutic efficacy in rheumatoid arthritis (RA). Nanostructured lipid carriers (NLCs) offer a promising strategy to overcome these limitations. **Methods:** Iguratimod-loaded NLCs were prepared by the ultra-sonication method using glyceryl monostearate (solid lipid), oleic acid (liquid lipid, 7:3 ratio), and Tween 20 (surfactant). A Box-Behnken design (13 runs) was employed to optimize three independent variables: total lipid concentration (X1: 1–3% w/v), surfactant concentration (X2: 0.5–1.5% w/v), and sonication time (X3: 10–20 seconds), evaluating particle size (R1), polydispersity index (R2), and percentage drug entrapment (R3). **Results:** The optimized formulation showed a particle size of 143.7 nm, PDI of 0.211, and entrapment efficiency of 73.24 ± 1.23%. Zeta potential was −19.1 ± 0.3 mV. FTIR and DSC studies confirmed no drug-excipient incompatibility. TEM revealed spherical particles with smooth surfaces. In vitro drug release demonstrated sustained release of 83.18 ± 1.36% over 30 hours. Stability studies over 3 months showed optimal stability at refrigerated (2–8°C) and room temperature conditions. **Conclusion:** The optimized Iguratimod-loaded NLCs exhibited excellent physicochemical characteristics, sustained release profile, and stability, representing a promising oral delivery system for RA treatment.

Keywords

Iguratimod, nanostructured lipid carriers, Box-Behnken design, rheumatoid arthritis, sustained release

*****

1. INTRODUCTION

Rheumatoid arthritis (RA) is a long-lasting, systemic inflammatory condition primarily impacting the joints and surrounding tissues, often resulting in substantial disability (Firestein & McInnes, 2017; Smolen et al., 2016). The global prevalence of RA ranges from 0.3% to 1%, with an estimated prevalence of about 0.75% in India (Smolen et al., 2016). The pathophysiology of RA is characterized by synovial cell proliferation, cartilage degeneration, and bone erosion, orchestrated by pro-inflammatory cytokines such as interleukin-1 (IL-1), interleukin-6

(IL-6), and tumor necrosis factor-alpha (TNF-α) (McInnes & Schett, 2007).

Iguratimod (IGU) is a small synthetic disease-modifying antirheumatic drug (csDMARD) widely used in Japan and China for rheumatoid arthritis, characterized by its immunomodulatory and anti-inflammatory mechanisms, including inhibition of nuclear factor-κB and suppression of pro-inflammatory cytokines (Tanaka et al., 2013; Gupta et al., 2024). Despite its therapeutic potential, IGU exhibits poor aqueous solubility (0.31 ± 0.76 mg/ml in distilled water) and low oral bioavailability, necessitating higher doses and leading to systemic side effects such as elevated transaminases, nausea, vomiting, and rashes (Brunton et al., 2025).

Nanostructured lipid carriers (NLCs) are second-generation lipid-based nanocarriers designed by blending solid lipids with liquid lipids, creating an imperfect crystalline structure that accommodates a higher drug load while preventing drug expulsion during storage (Müller et al., 2002). NLCs have been consistently reported to provide increased entrapment efficiency due to the structural parity of two lipids, resulting in imperfections that provide higher space for drug accommodation (Mall et al., 2025). The present study aimed to formulate, optimize using Box-Behnken design, and comprehensively characterize Iguratimod-loaded NLCs for improved RA therapy.

2. MATERIALS AND METHODS

2.1 Materials

Iguratimod was obtained from Dr. Reddy's Laboratory Ltd., Hyderabad. Glyceryl monostearate (GMS), glyceryl palmitostearate, and glyceryl behenate were procured from Gattefosse India Pvt. Ltd., Mumbai. Oleic acid, Tween 20, Tween 80, PEG 400, and other chemicals were purchased from S.D. Fine chemicals, Mumbai.

2.2 Identification and Characterization of Drug

2.2.1 Organoleptic properties and melting point

The organoleptic characteristics of Iguratimod were evaluated through visual inspection. Iguratimod appeared as an odorless, white to off-white solid powder. The melting point was determined using the capillary tube method and found to be 239 ± 0.5°C, matching the standard value (Indian Pharmacopoeia Commission, 2022).

2.2.2 UV spectrophotometric analysis and calibration curve

The absorbance maximum (λ_{max}) for Iguratimod was identified by scanning a 100 µg/ml solution in distilled water within a wavelength range of 200-400 nm using a double-beam UV-visible spectrophotometer (Genesys 180, Thermo Fisher Scientific, USA). The λ_{max} was found to be 257.16 nm. Calibration curves were prepared in distilled water and phosphate buffer pH 6.8 over a concentration range of 10–100 µg/ml, showing linearity with correlation coefficients >0.99.

2.2.3 Solubility determination

The saturated solubility of Iguratimod was assessed using the saturation solubility method (Higuchi & Connors, 1965). An excess amount of Iguratimod was added to glass vials containing 10 ml of distilled water, phosphate buffer pH 6.8, or dimethyl sulfoxide (DMSO). After 72 hours of mechanical agitation, samples were centrifuged, filtered, and analyzed at 257.16 nm. Iguratimod showed low aqueous solubility: 0.31 ± 0.76 mg/ml in distilled water and 0.24 ± 0.49 mg/ml in phosphate buffer pH 6.8, but high solubility in DMSO (15.05 ± 0.14 mg/ml).

2.2.4 Drug-excipient compatibility study (FTIR and DSC)

Fourier transform infrared (FTIR) spectra for Iguratimod, glyceryl monostearate, oleic acid, tween-20, and their physical mixtures were recorded using an FTIR spectrophotometer (Bruker, Germany) over the wavelength range from 4000 to 400 cm^{-1} (Silverstein et al., 2014). The FTIR spectra of Iguratimod, GMS, oleic acid, Tween 20, and the physical mixture, respectively. The major peaks of Iguratimod were present in the physical mixture spectrum, confirming no incompatibility.

Differential scanning calorimetry (DSC) thermograms were obtained separately for all samples using a DSC-60 (Shimadzu, Japan) at a heating rate of 10°C per minute over temperatures ranging from 30 to 400°C under an inert nitrogen atmosphere (40 ml/min) (Pavia et al., 2019). The DSC thermograms of Iguratimod showed a sharp endothermic peak at 238.45°C, indicating its melting point and crystalline nature. The physical mixture showed two small endothermic peaks at 65.12°C (GMS) and 238.45°C (drug), confirming the absence of incompatibility.

2.3 Preliminary Screening of Materials

2.3.1 Selection of solid lipid

The partitioning behavior of Iguratimod into melted lipid phases was studied following the method of Patel et al. (2017). Lipid (200 mg each of GMS, glyceryl palmitostearate, and glyceryl behenate) was heated to 60–70°C, and 10 mg of Iguratimod was added. After adding 5 ml of heated distilled water and stirring for 30 minutes, the mixture was filtered, and the filtrate was analyzed at 257.1 nm. Glyceryl monostearate showed the highest drug partitioning and was selected as the solid lipid.

2.3.2 Selection of liquid lipid

Liquid lipid (2 ml each of Capmul MCM, oleic acid, and Labrafil) was taken in vials, and Iguratimod was

added incrementally with continuous shaking (Beloqui et al., 2016). After ultracentrifugation (10,000 rpm, 10 min), the sediment was analyzed. Oleic acid exhibited maximum drug partitioning and was selected as the liquid lipid.

2.3.3 Selection of surfactant

An excessive amount of Iguratimod (~20 mg) was added to 1 ml of surfactants (Tween 20, Tween 80, and PEG 400) and shaken for 72 h at 25°C (Müller et al., 2002). After centrifugation (10,000 rpm, 5 min), the supernatant was analyzed. Tween 20 showed the highest drug solubility and was selected as the surfactant.

2.4 Formulation of Iguratimod-Loaded NLCs

Iguratimod-loaded NLCs were formulated using the ultra-sonication method (Jin et al., 2018). GMS and oleic acid (7:3 ratio, 1–3% w/v) were melted at 70°C, and Iguratimod (20 mg) was added. Simultaneously, Tween 20 (0.5–1.5% w/v) dispersed in distilled water (20 ml) was heated to the same temperature. The hot aqueous phase was added to the melted lipid phase and stirred at 1000 rpm for 30 minutes. This hot dispersion was sonicated at 80% amplitude for 1 cycle using a probe sonicator (Labsonic M, Germany) and then allowed to cool to room temperature to obtain drug-loaded NLCs.

2.5 Box-Behnken Optimization

The optimization of Iguratimod-loaded NLCs was conducted using a Box-Behnken design facilitated by Design-Expert® software (version 23.1.6.0) (Zhang et al., 2015). The design information. Three independent variables were selected: total lipid concentration (X1: 1, 2, 3% w/v), surfactant concentration (X2: 0.5, 1, 1.5% w/v), and sonication time (X3: 10, 15, 20 seconds). The response variables included particle size (R1, nm), polydispersity index (R2), and percentage drug entrapment (R3, %). A total of 13 runs were prepared in randomized order as per the experimental framework. Statistical significance was assessed through ANOVA, and 3D response surface plots were generated.

2.6 Characterization of Iguratimod-Loaded NLCs

2.6.1 Particle size, polydispersity index, and zeta potential

The average particle size and PDI of NLCs were determined using a Malvern Zetasizer Nano-ZS (Malvern Instruments, UK) at 25°C. All samples were diluted 10 times with double-distilled and filtered (0.2 µm) water for measurement (Müller et al., 2002). Zeta potential was measured using the same instrument to assess the physical stability of colloidal dispersions.

2.6.2 Percentage drug entrapment

Percentage drug entrapment was determined using the Sephadex G-50 column method (Beloqui et al., 2016). NLC dispersion was passed through a saturated Sephadex G-50 column, and the elute was collected. The eluted fraction was mixed with a small amount of DMSO to dissolve the lipidic fraction, diluted with distilled water, and analyzed using a UV spectrophotometer at 257.16 nm.

2.6.3 *In vitro* drug release study

Cumulative in vitro percentage drug release of optimized Iguratimod-loaded NLCs was determined using the dialysis bag diffusion technique with phosphate buffer pH 6.8 (500 ml) as the release medium (Jin et al., 2018). NLC dispersion (equivalent to 10 mg of drug) was placed in a dialysis bag (cut-off 14000, HIMEDIA, Mumbai), which was then immersed in the receptor compartment containing the diffusion medium stirred at 50 rpm at 37 ± 0.5°C. Samples (5 ml) were withdrawn at regular time intervals and replaced with fresh medium. The samples were analyzed using a UV-visible spectrophotometer to determine the concentration of Iguratimod.

2.6.4 Transmission electron microscopy (TEM)

TEM analysis of the optimized NLC formulation was carried out to understand the shape and surface morphology (Zhang et al., 2015). A drop of Iguratimod-loaded NLC dispersion with 0.01% phosphotungstic acid was placed on a carbon film coated on a copper grid. The copper grid was placed into the sample holder, fixed in a vacuum chamber, and images were recorded at 80 kV using a Philips Technai-20 (Japan).

2.6.5 Stability study

Stability was determined by storing the optimized Iguratimod-loaded NLC dispersion at three different storage conditions: in a refrigerator (2–8°C), at room temperature (25–28°C), and at higher temperature (45–50°C) for up to 3 months (Puglia & Blasi, 2016). Samples were collected at 1-month intervals and analyzed for particle size, zeta potential, and percentage drug entrapment.

3. RESULTS AND DISCUSSION

3.1 Box-Behnken Design Optimization

The 13 formulations (NLCs-1 to NLCs-13) were prepared according to the experimental design. Table 1 illustrates the impact of independent variables on the response variables. A linear model was identified as the most suitable fit for all three response variables.

Table 1: Effect of independent variables on response variables

Batch No.	Independent variable			Response variables		
	(X1) % w/v	(X2) % w/v	(X3) seconds	(R1)	(R2)	(R3)
NLCs-1	3	0.5	15	157.87	0.245	76.45
NLCs-2	1	0.5	15	149.53	0.216	71.43
NLCs-3	3	1	10	152.18	0.239	79.29
NLCs-4	2	1	15	150.71	0.231	73.44
NLCs-5	2	1.5	20	148.29	0.225	73.45
NLCs-6	1	1	10	146.94	0.217	71.41
NLCs-7	3	1	20	151.16	0.244	79.29
NLCs-8	2	1.5	10	149.07	0.228	76.59
NLCs-9	2	0.5	10	150.26	0.232	74.33
NLCs-10	1	1.5	15	144.76	0.211	71.76
NLCs-11	1	1	20	143.19	0.213	70.57
NLCs-12	2	0.5	20	147.53	0.227	75.41
NLCs-13	3	1.5	15	150.04	0.242	77.64

3.1.1 Effect of independent variables on particle size

The influence of independent variables on particle size was assessed and illustrated through a 3D surface plot presented in **Figure 1**. Particle sizes ranged from 143.19 nm (NLCs-11) to 157.87 nm (NLCs-1). Increasing surfactant concentration and sonication time decreased particle size, while increasing total lipid concentration slightly increased particle size. The optimized particle size was determined to be **143.7 nm** (**Table 2**). A summary of the statistical outcomes from the ANOVA test for particle size is presented in **Table 3** (R^2 = 0.8112, adjusted R^2 = 0.7482, predicted R^2 = 0.6062, SD = 1.54, % CV = 1.04).

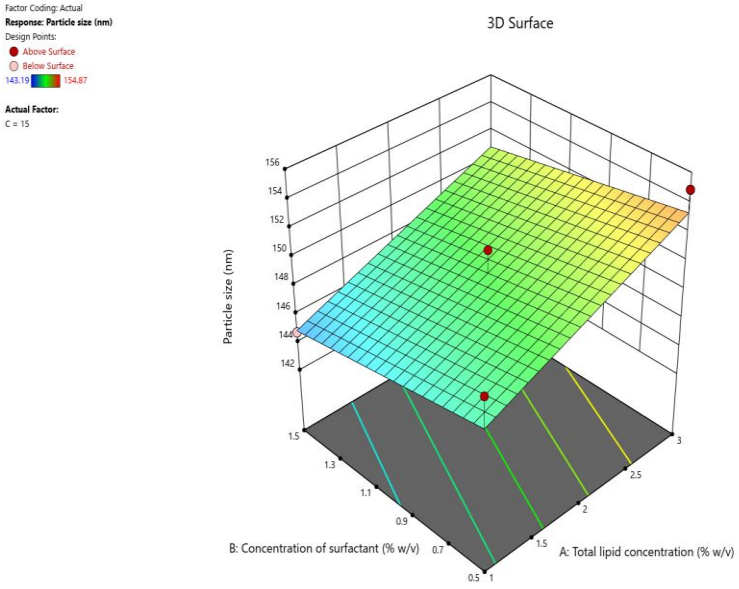

Figure 1: 3D surface plot of effect of independent variables on particle size

Table 2: Validated values of independent variables and response variables for NLCs

Type of Variable	Variables	Optimized Value	Validated Value (n=3)
Independent	Total lipid concentration (% w/v)	1.834	1.834
	Concentration of surfactant (% w/v)	1.5	1.5
	Sonication time (Seconds)	20	20
Response or Dependent	Particle size (nm)	146.33	143.7
	Polydispersity index	0.223	0.211
	Percentage drug entrapment (%)	73.99	73.24

Table 3: Summary of statistical data of ANOVA for particle size

Formulations	R^2	Adjusted R^2	Predicted R^2	SD	% CV
NLCs	0.8112	0.74822	0.6062	1.54	1.04

3.1.2 Effect of independent variables on polydispersity index

The impact of independent variables on the PDI was assessed and illustrated through a 3D surface plot as depicted in **Figure 2**. PDI values ranged from 0.211 (NLCs-10) to 0.245 (NLCs-1). Increased surfactant concentration and sonication time reduced the PDI, while variations in total lipid concentration did not produce any notable effect. The optimized PDI value was recorded at **0.211** (**Table 4**). **Table 5** summarizes the statistical data (R^2 = 0.9722, adjusted R^2 = 0.9722, predicted R^2 = 0.9630, SD = 0.0023, % CV = 0.9947).

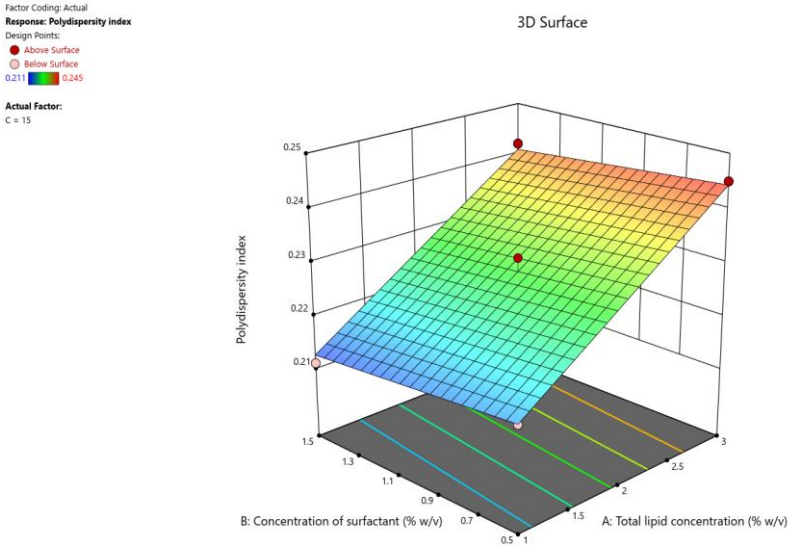

Figure 2: 3D surface plot of effect of independent variables on polydispersity index

Table 4: Validated values of independent variables and response variables for NLCs

Type of Variable	Variables	Optimized Value	Validated Value (n=3)
Independent	Total lipid concentration (% w/v)	1.834	1.834
	Concentration of surfactant (% w/v)	1.5	1.5
	Sonication time (Seconds)	20	20
Response or Dependent	Particle size (nm)	146.33	143.7
	Polydispersity index	0.223	0.211
	Percentage drug entrapment (%)	73.99	73.24

Table 5: Summary of statistical data of ANOVA for polydispersity index

Formulations	R^2	Adjusted R^2	Predicted R^2	SD	% CV
NLCs	0.9722	0.9722	0.9630	0.0023	0.9947

3.1.3 Effects of independent variables on percentage drug entrapment

The effects of independent variables on percentage drug entrapment were determined and recorded as a 3D surface plot shown in **Figure 3**. Entrapment efficiency ranged from 70.57% (NLCs-11) to 79.29% (NLCs-3 and NLCs-7). Increased total lipid concentration and increased surfactant concentration enhanced entrapment. The optimized percentage drug entrapment was found to be **73.24 ± 1.23%** (**Table 6**). **Table 7** presents the summary of statistical data (R^2 = 0.8854, adjusted R^2 = 0.8472, predicted R^2 = 0.7621, SD = 1.18, % CV = 1.57).

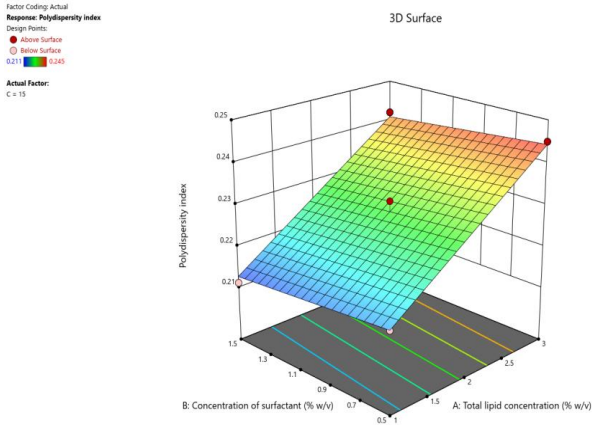

Figure 3: 3D surface plot of effect of independent variables on percentage drug entrapment

Table 6: Validated values of independent variables and response variables for NLCs

Type of Variable	Variables	Optimized Value	Validated Value (n=3)
Independent	Total lipid concentration (% w/v)	1.834	1.834
	Concentration of surfactant (% w/v)	1.5	1.5
	Sonication time (Seconds)	20	20
Response or Dependent	Particle size (nm)	146.33	143.7
	Polydispersity index	0.223	0.211
	Percentage drug entrapment (%)	73.99	73.24

Table 7: Summary of statistical data of ANOVA for percentage drug entrapment

Formulations	R^2	Adjusted R^2	Predicted R^2	SD	% CV
NLCs	0.8854	0.8472	0.7621	1.18	1.57

3.1.4 Optimized formulation validation

Based on the findings from the Box-Behnken design, the optimized values for both independent and dependent variables were determined. **Table 6** presents the validated results for NLCs. The validated response variable values were similar to the optimized values, confirming the reliability of the statistical model.

3.2 Particle Size and Polydispersity Index Analysis

The particle size and PDI of all batches of Iguratimod-loaded NLCs are shown in **Table 8** The optimized formulation showed a particle size of 143.7 nm and PDI of 0.211. **Figure 4** shows the particle size distribution image of the optimized formulation. The results revealed the presence of low-size monodispersed particles in the NLC dispersion, which is desirable for uniform drug delivery and consistent in vivo performance (Danaei et al., 2018).

Table 8: Particle size and PDI values of Iguratimod loaded NLCs (n=3)

S. No.	Batch No.	Particle Size (Z avg in nm ± SEM)	PDI
1	NLCs-1	157.87±0.2	0.245±0.03
2	NLCs-2	149.53±0.3	0.216±0.09
3	NLCs-3	152.18±0.2	0.239±0.06
4	NLCs-4	150.71±0.4	0.231±0.08
5	NLCs-5	148.29±0.1	0.225±0.05
6	NLCs-6	146.94±0.3	0.217±0.04
7	NLCs-7	151.16±0.5	0.244±0.07
8	NLCs-8	149.07±0.2	0.228±0.09
9	NLCs-9	150.26±0.7	0.232±0.03
10	NLCs-10	144.76±0.5	0.211±0.11
11	NLCs-11	143.19±0.3	0.213±0.05

12	NLCs-12	147.53±0.8	0.227±0.09
13	NLCs-13	150.04±0.4	0.242±0.08
14	Optimized	142.39±0.2	0.212±0.05

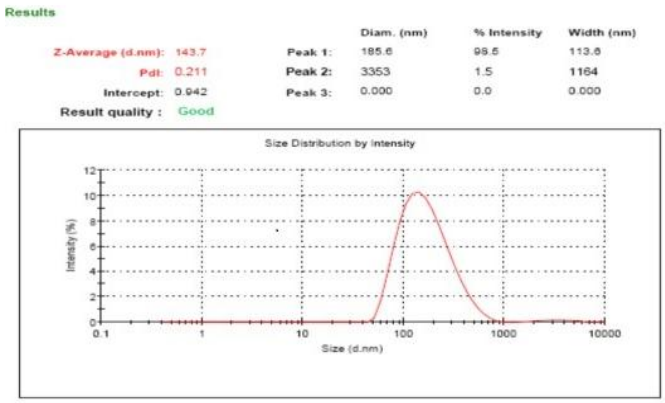

Figure 4: Particle size distribution of optimized Iguratimod loaded NLCs

3.3 Zeta Potential

The zeta potential of all batches of Iguratimod-loaded NLCs is shown in **Table 9**. The zeta potential of the optimized formulation was found to be **−19.1 ± 0.3 mV** (**Figure 5**). The high absolute value of zeta potential (greater than ±15 mV) indicated good electrostatic stability of the NLC formulation, preventing particle aggregation through electrostatic repulsion (Müller et al., 2002).

Table 9: Zeta potential of Iguratimod loaded NLCs (n=3)

S. No.	Batch No.	Zeta potential (mV±SEM)
1	NLCs-1	-18.4±0.1
2	NLCs-2	-17.6±0.2
3	NLCs-3	-19.5±0.5
4	NLCs-4	-14.7±0.4
5	NLCs-5	-18.2±0.3
6	NLCs-6	-17.5±0.2
7	NLCs-7	-18.8±0.4
8	NLCs-8	-17.9±0.2
9	NLCs-9	-18.5±0.4
10	NLCs-10	-19.1±0.1
11	NLCs-11	-18.9±0.3
12	NLCs-12	-18.3±0.3
13	NLCs-13	-17.8±0.4
14	Optimized	-19.1±0.3

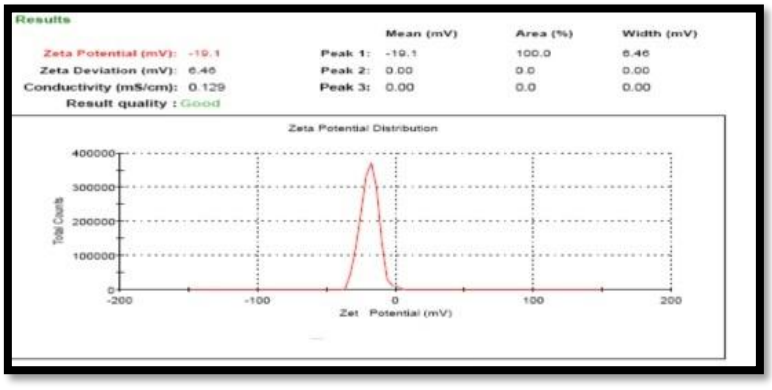

Figure 5: Zeta potential of optimized Iguratimod loaded NLCs

3.4 Percentage Drug Entrapment

The percentage drug entrapment of all batches is presented in **Table 10**. The optimized formulation showed an entrapment efficiency of **73.24 ± 1.23%**. The high entrapment efficiency is attributed to the structural imperfections in the NLC matrix created by blending solid and liquid lipids, providing higher space for drug accommodation (Mall et al., 2025). Additionally, the higher solubility of Iguratimod in the liquid lipid (oleic acid) contributed to the enhanced payload capacity.

Table 10: Percentage drug entrapment of Iguratimod loaded NLCs (n=3)

S. No.	Batch No.	Percentage drug entrapment (%±SEM)
1	NLCs-1	71.43±1.04
2	NLCs-2	79.29±1.37
3	NLCs-3	73.44±0.98
4	NLCs-4	73.45±1.26
5	NLCs-5	71.41±1.16
6	NLCs-6	79.29±1.23
7	NLCs-7	76.59±1.18
8	NLCs-8	74.33±1.51
9	NLCs-9	71.76±1.23
10	NLCs-10	70.57±1.73
11	NLCs-11	75.41±0.94
12	NLCs-12	77.64±1.07
13	NLCs-13	71.43±1.38
14	Optimized	74.39±1.01

3.5 In Vitro Drug Release Study

The cumulative in vitro drug release data of the optimized Iguratimod-loaded NLCs are presented in **Table 11** and **Figure 6**. The formulation showed a biphasic release pattern characterized by an initial burst release (5.20% at 1 hour) followed by prolonged sustained release, reaching **83.18 ± 1.36% at 30 hours**. The sustained release is attributed to the solid lipid matrix, which controls drug diffusion. The initial burst release may be due to the presence of drug adsorbed on the nanoparticle surface or dissolved in the liquid lipid component (Jin et al., 2018). This release profile is particularly beneficial for chronic inflammatory conditions like RA, as it maintains therapeutic drug levels over extended durations while reducing dosing frequency (Beloqui et al., 2016).

Table 11: Cumulative *in-vitro* % drug release data of optimized Iguratimod loaded NLCs (n=3)

Time (Hours)	Cumulative *in-vitro* % drug release (%±SEM)
0	0
1	5.20±0.32
2	9.33±1.10
3	13.11±1.22
4	18.22±1.45
5	20.72±1.56
6	23.84±1.81
7	28.65±1.32
8	33.58±1.11
9	39.19±1.48
10	44.83±1.71
24	75.10±1.48
30	83.18±1.36

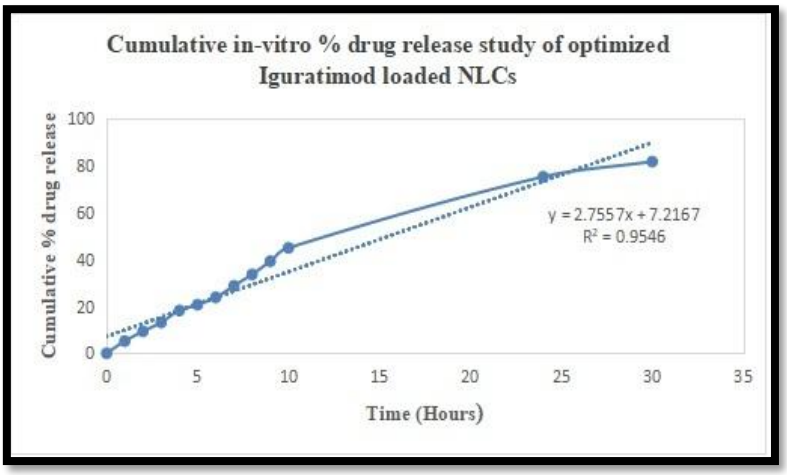

Figure 6: Cumulative *n-vitro* % drug release data of optimized Iguratimod loaded NLCs

3.6 Shape and Surface Morphology Using TEM

The TEM image of Iguratimod-loaded NLCs is shown in **Figure 7**. The image indicated smooth surfaces and spherical shapes of the particles, with a size range of up to 140–150 nm, which was consistent with the DLS measurements. The spherical morphology is advantageous for cellular uptake and biodistribution (Zhang et al., 2015).

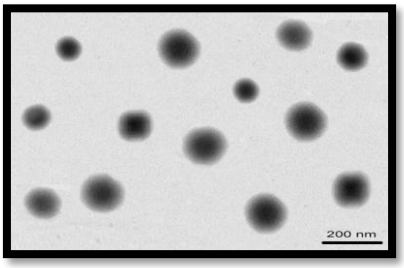

Figure 7: TEM image of optimized Iguratimod loaded NLCs

3.7 Stability Study

The stability study data for the optimized Iguratimod-loaded NLCs are presented in **Table 12**. The formulation exhibited the highest stability when stored in refrigerated conditions (2–8°C) and at room temperature (25–28°C) for up to 3 months. Under refrigerated conditions, particle size increased from 142.39 ± 0.2 nm to 148.81 ± 0.3 nm, zeta potential changed from −19.1 ± 0.2 mV to −18.4 ± 0.3 mV, and entrapment decreased from 74.39 ± 1.01% to 71.04 ± 0.59%. At room temperature, similar stability was observed. However, at elevated temperatures (45–50°C), a slight decrease in stability was observed, with particle size increasing to 159.21 ± 0.2 nm and entrapment decreasing to 66.48 ± 0.39% after 3 months. These findings are consistent with previous reports that NLCs maintain physical stability during storage due to the absence of polymorphic transitions (Müller et al., 2002).

Table 12: Stability data of optimized Iguratimod loaded NLCS (n=3)

Sampling Time	Storage conditions for optimized Iguratimod loaded NLCs		
	Refrigerated condition (2-8 ℃)	Room temperature (25-28 ℃)	Higher temperature (45-50 ℃)
	Particle size (nm)		
Initial	142.39±0.2	142.39±0.2	142.39±0.2
After 1months	144.79±0.3	142.71±0.3	146.27±0.3
After 2months	146.63±0.5	143.39±0.3	150.39±0.3
After 3months	148.81±0.3	144.87±0.3	159.21±0.2

Zeta potential (mV)			
Initial	-19.1±0.2	-19.1±0.2	-19.1±0.2
After 1months	-19.0±0.2	-19.1±0.2	-17.4±0.2
After 2months	-18.7±0.2	-18.8±0.3	-16.3±0.2
After 3months	-18.4±0.3	-18.6±0.3	-16.1±0.3
Percentage drug entrapment (%)			
Initial	74.39±1.01	74.39±1.01	74.39±1.01
After 1months	73.29±0.39	73.28±0.37	72.19±1.11
After 2months	72.10±0.46	73.11±0.17	68.28±0.84
After 3months	71.04±0.59	72.47±0.28	66.48±0.39

4. CONCLUSION

Iguratimod-loaded NLCs were successfully formulated using the ultra-sonication method and systematically optimized using a Box-Behnken design. The optimized formulation achieved a particle size of 143.7 nm, PDI of 0.211, entrapment efficiency of 73.24 ± 1.23%, and zeta potential of −19.1 ± 0.3 mV. FTIR and DSC studies confirmed the absence of drug-excipient incompatibility. TEM revealed spherical particles with smooth surfaces. In vitro release studies demonstrated sustained release of 83.18 ± 1.36% over 30 hours, indicating a biphasic release pattern suitable for chronic RA management. Stability studies confirmed good stability for 3 months under refrigerated and room temperature conditions. This formulation strategy effectively addresses the poor solubility and bioavailability limitations of Iguratimod, offering a promising approach for improved rheumatoid arthritis therapy. Future studies should focus on scale-up, long-term stability, and in vivo pharmacokinetic evaluations.

REFERENCES

Beloqui, A., Solinís, M. Á., Rodríguez-Gascón, A., Almeida, A. J., & Préat, V. (2016). Nanostructured lipid carriers: Promising drug delivery systems for future clinical use. *Journal of Controlled Release*, 243, 1–15.

Brunton, L. L., Hilal-Dandan, R., & Knollmann, B. C. (Eds.). (2025). *Goodman & Gilman's The pharmacological basis of therapeutics* (14th ed.). McGraw-Hill.

Danaei, M., Dehghankhold, M., Ataei, S., Hasanzadeh Davarani, F., Javanmard, R., Dokhani, A., Khorasani, S., & Mozafari, M. R. (2018). Impact of particle size and polydispersity index on the clinical applications of lipidic nanocarrier systems. *Pharmaceutics*, 10(2), 57.

Firestein, G. S., & McInnes, I. B. (2017). Immunopathogenesis of rheumatoid arthritis. *Immunity*, 46(2), 183–196.

Gupta, N., Begum, S., Farooqui, V., Afreen, S., & Avunoori, P. (2024). A review on Iguratimod: Bridging hope for arthritis patients through the dual power of immunomodulation and anti-inflammation. *Asian Journal of Immunology*, 7(1), 79–89.

Higuchi, T., & Connors, K. A. (1965). Phase solubility techniques. *Advances in Analytical Chemistry and Instrumentation*, 4, 117–212.

Indian Pharmacopoeia Commission. (2022). *Indian Pharmacopoeia*. Indian Pharmacopoeia Commission.

Jin, Y., Li, S., Fu, J., Li, X., & Wang, R. (2018). Preparation, characterization and evaluation of drug-loaded NLCs for enhanced oral bioavailability of poorly soluble drugs. *Journal of Drug Delivery Science and Technology*, 45(Pt B), 410–419.

Mall, J., Naseem, N., Haider, M. F., Rahman, M. A., Khan, S., & Siddiqui, S. N. (2025). Nanostructured lipid carriers as a drug delivery system: A comprehensive review with therapeutic applications. *Intelligent Pharmacy*, 3(4), 243–255.

McInnes, I. B., & Schett, G. (2007). Cytokines in the pathogenesis of rheumatoid arthritis. *Nature Reviews Immunology*, 7(6), 429–442.

Müller, R. H., Radtke, M., & Wissing, S. A. (2002). Solid lipid nanoparticles (SLN) and nanostructured lipid carriers (NLC) in cosmetic and pharmaceutical dermal products. *International Journal of Pharmaceutics*, 242(1–2), 121–128.

Patel, R., Patel, M., & Rajesh, K. S. (2017). Selection of lipid and solid lipid nanoparticles: Impact on drug delivery. *International Journal of Pharmaceutical Sciences Review and Research*, 45(1), 107–116.

Pavia, D. L., Lampman, G. M., Kriz, G. S., & Vyvyan, J. R. (2019). *Introduction to thermal analysis: DSC, TGA and related techniques* (2nd ed.). Cengage Learning.

Puglia, C., & Blasi, P. (2016). Nanostructured lipid carriers (NLC) as delivery systems for poorly soluble drugs: Recent advances and perspectives. *Drug Delivery*, 23(8), 2866–2878.

Silverstein, R. M., Webster, F. X., Kiemle, D. J., & Bryce, D. L. (2014). *Spectrometric identification of organic compounds* (8th ed.). John Wiley & Sons.

Smolen, J. S., Aletaha, D., & McInnes, I. B. (2016). Rheumatoid arthritis. *Lancet*, 388(10055), 2023–2038.

Tanaka, Y., Takeuchi, T., Miyasaka, N., & Koike, T. (2013). Iguratimod: A new disease-modifying antirheumatic drug. *Journal of Immunology*, 191(10), 4969–4978.

Zhang, Q., Wang, H., Chen, L., Wei, W., & Yuan, W. (2015). Quality by Design (QbD) based development and optimization of nanostructured lipid carriers for improved oral bioavailability. *International Journal of Pharmaceutics*, 484(1–2), 148–158.